



1 **Comparing the spatial patterns of climate change in the 9th and 5th millennia B.P. from**
2 **TRACE-21 model simulations**

3

4 **Liang Ning^{1,2,3}, Jian Liu^{1,2*}, Raymond S. Bradley³, and Mi Yan^{1,2}**

5 ¹Key Laboratory of Virtual Geographic Environment, Ministry of Education; State key Laboratory
6 of Geographical Environment Evolution, Jiangsu Provincial Cultivation Base; School of
7 Geographical Science, Nanjing Normal University, Nanjing, 210023, China

8 ²Jiangsu Center for Collaborative Innovation in Geographical Information Resource Development
9 and Application, Nanjing, 210023, China

10 ³Climate System Research Center, Department of Geosciences, University of Massachusetts,
11 Amherst, 01003, United States

12 *jliu@njnu.edu.cn

13

14 **ABSTRACT**

15 The spatial patterns of global temperature and precipitation changes, as well as corresponding
16 large-scale circulation patterns during the latter part of the 9th and 5th millennia B.P. (4800-4500
17 versus 4500-4000 years B.P. and 9200-8800 versus 8800-8000 years B.P.) are compared through
18 a group of transient simulations using Community Climate System Model version 3 (CCSM3).
19 Both periods are characterized by significant sea surface temperature decreases over the North
20 Atlantic south of Iceland. Temperatures were also colder across the northern hemisphere, but
21 warmer in the southern hemisphere. Significant precipitation decreases are seen over most of the
22 northern hemisphere, especially over Eurasia and the Asian monsoon regions, indicating a weaker
23 summer monsoon. Large precipitation anomalies over northern South America and adjacent ocean
24 regions are related to a southward displacement of the Inter Tropical Convergence Zone (ITCZ).
25 Climate changes in the late 9th millennium B.P. (“The 8.2ka BP event”) are widely considered to
26 have been caused by a large fresh water discharge into the northern Atlantic, which is confirmed
27 in a meltwater forcing sensitivity experiment, but this was not the cause of changes occurring
28 between the early and latter half of the 5th millennium B.P. We speculate that long-term changes
29 in insolation related to precessional forcing led to cooling, which passed a threshold around 4500
30 years B.P., leading to a reduction in the Atlantic meridional overturning circulation (AMOC) and
31 associated teleconnections across the globe. The onset of the Neoglacial occurred around this time,



32 and the subsequent changes in glacierization have persisted, modulated by internal centennial-
33 scale ocean-atmosphere variability. We suggest that the “4.2ka B.P. event” was one of several late
34 Holocene multi-century fluctuations that were embedded in a longer-term, lower frequency change
35 in climate, linked to orbital forcing.

36

37 **1. Introduction**

38 It is well-documented that the first order driver of Holocene climate change was orbital
39 forcing, with an overall decline in summer insolation in summer months, particularly at high
40 latitudes. This led to a drop in temperatures at high latitudes and less rainfall throughout the
41 monsoon regions of the northern hemisphere, as seen in many paleoclimatic records (Burns, 2011;
42 Solomina et al., 2015). Shorter-term rainfall fluctuations around this long-term change in
43 hydrological conditions are clearly seen in many speleothem and lacustrine sediment records (e.g.
44 Wang et al., 2005; Kathayat et al., 2017). Abrupt hydrological changes around 4.2 ka BP have
45 been documented for various regions of the world (Weiss, 2016). For example, based on a variety
46 of physical and biological proxies, Booth et al. (2005) found a severe drought that affected the
47 mid-continent of North America between 4.1 and 4.3 ka BP. Over eastern Asia, Tan et al. (2018)
48 found that there were droughts over the northern part of eastern China while floods occurred over
49 the southern part around 4.2 ka BP. It was suggested that these climate changes may have been
50 global in extent (Bond et al., 2001; Thompson et al., 2002; Booth et al., 2005).

51 In recent years, a more comprehensive picture of the 4.2 ka BP event has been derived
52 from analysis of new high-resolution proxy data from different regions, and the event has become
53 the focus of several symposia and research conferences (Weiss, 2016). This event is of particular
54 interest as it is associated with societal collapse and regional abandonment in many different
55 regions. For example, the collapse and abandonment of Akkadian imperial settlements in the
56 Khabur Plains, and other communities in dry farming domains across the Aegean and West Asia,
57 was in response to the abrupt nature with which the megadrought began (with its onset in less than
58 five years), its magnitude (a precipitation reduction of 30-50%) and its long duration (200-300
59 years) (Weiss, 2015).

60 Although a drought episode around 4.2ka B.P. has been found in many proxy
61 reconstructions, the mechanisms that brought this about are still unclear though different
62 hypotheses have been proposed. For example, Staubwasser and Weiss (2006) suggested that the



63 abrupt climate change event at 4.2ka B.P., as well as other widespread droughts around 8.2ka BP
64 and 5.2ka BP over the eastern Mediterranean, West Asia, and the Indian subcontinent, were caused
65 by a change in subtropical upper-level flow over the eastern Mediterranean and Asia. Weiss (2016)
66 also suggested that the major global monsoon and ocean-atmosphere circulation systems were
67 deflected or weakened synchronously at 4.2ka BP, causing major century-scale precipitation
68 disruptions (severe megadroughts) over different regions. Other studies (Wang et al., 2005; Tan
69 et al., 2018) have also noted weakening of the Asian summer monsoon at around this time,
70 resulting in drought over the northern part of eastern China and flooding over the southern part.

71 Some studies have suggested that these large-scale circulation anomalies may be induced
72 by persistent modes of internal climate variability, though there is a wide range of explanations.
73 For example, Booth et al. (2005) indicated that the widespread mid-latitude and subtropical
74 drought around 4.2ka BP was linked to a La Niña-like SST pattern, possibly associated with
75 amplification of this spatial mode by variations in solar irradiance or volcanism. On the other
76 hand, Hong et al. (2005) analyzed a 12000-yr proxy record for the East Asian monsoon and
77 concluded that such abnormal climate conditions could possibly result from frequent and severe
78 El Niño activities. Using paired oxygen isotope records from North America, Liu et al. (2014b)
79 indicated that there was a transition from a negative Pacific North American (PNA)-like pattern
80 during the mid-Holocene to a positive PNA-like pattern during the late Holocene, which led to
81 drier conditions in northwestern North America. A similar conclusion was reached by
82 Finkenbinder et al. (2016) based on lake sediment records from Newfoundland. They argued that
83 this transition took place around 4.3ka B.P., leading to wetter conditions across the Newfoundland
84 region. In contrast, Bond et al. (2001) argued that North Atlantic SST anomalies around 4.2ka
85 B.P. were related to the North Atlantic Oscillation (NAO) pattern. Deininger et al. (2017) also
86 found that changes in the atmospheric circulation associated with northward and southward
87 propagating westerlies (similar to the NAO but on a millennial instead of decadal scale) could be
88 a possible driver of coherency and cyclicity during the last 4.5ka BP, as seen in multiple
89 speleothem $\delta^{18}\text{O}$ records that span most of the European continent. However, the ultimate driver
90 for this oscillation remains unclear.

91 Wang (2009a) reviewed studies of Holocene cold events, and concluded that an outburst
92 flood in which pro-glacial Lake Agassiz drained a large volume of freshwater into the North
93 Atlantic extremely rapidly (Bianchi and McCave, 1999; Risebrobakken et al., 2003; McManus et



94 al., 2004; Clarke et al., 2004) initiated the cold 8.2ka BP event, leading to a brief reorganization
95 of the North Atlantic Meridional Overturning Circulation (AMOC). Potential external forcing
96 factors for the 4.2ka BP event include non-linear responses to Milankovitch forcing, solar
97 irradiance variations, and explosive volcanic eruptions, all of which may have brought about
98 variations in the ocean-atmosphere system (Booth et al., 2005). Wang (2009a) concluded that
99 solar irradiance minima were the main cause of cold events in the mid- to late Holocene (including
100 the 4.2ka BP event) and that oscillations within the climate system could possibly have intensified
101 these cold events under certain circumstances (Wang, 2009b). Bond et al. (2001) also proposed a
102 possible link between the 4.2ka BP event and reduced solar radiation at that time.

103 In summary, the 8.2ka BP event and corresponding shifts in the ITCZ were caused by
104 glacial flooding of the North Atlantic and this can be reasonably simulated by coupled GCMs with
105 different boundary conditions and freshwater forcings (Alley and Agustsdottir, 2005; LeGrande et
106 al., 2006). At 4.2ka B.P., the major global monsoon and ocean-atmosphere circulation systems
107 may have been deflected or weakened synchronously, causing major century-scale precipitation
108 disruptions, resulting in severe megadroughts over many different regions (Weiss, 2016).
109 However, the forcing mechanisms that brought about the 4.2ka BP event are currently uncertain.
110 GCM simulations of the 4.2ka BP event have not received much attention, therefore, in this study,
111 the spatial patterns and corresponding mechanisms relevant to the 4.2 ka BP event and 8.2ka BP
112 event are compared.

113

114 **2. Data and methodology**

115 The simulations of the last 21ka (TRACE-21) were used in this study (He, 2011; He et al. 2013).
116 These transient simulations have been completed using Version 3 of the Community Climate
117 System Model (CCSM3), which is a coupled atmosphere-ocean general circulation model
118 developed by National Center for Atmospheric Research (NCAR). The atmosphere model in the
119 CCSM3 is the Community Atmospheric Model 3 (CAM3) with a horizontal resolution $\sim 3.75^\circ$
120 (T31), and the ocean model is the Parallel Ocean Program (POP) with a longitudinal resolution of
121 3.6° and variable latitudinal resolution. The “full-forcing” TRACE-21 simulation includes
122 changes in orbital parameters, greenhouse gases, ice extent (based on the ICE 5G-VM2
123 configurations) and meltwater fluxes from the Northern Hemisphere and Antarctic ice sheets.
124 Simulations in which only one of these factors was included have also been carried out and are



125 available in the TRACE-21 archive (Otto-Bliesner et al., 2006). These simulations can reproduce
126 the timing and magnitude of many aspects of climate evolution during the last 21 ka, such as sea
127 surface temperature (SST) (He et al., 2013). However, there are significant differences between
128 the rate of temperature change in the model during the early Holocene and many paleoclimatic
129 records (Liu et al., 2014a; Marcott et al., 2013). In this study, we do not address this enigma, but
130 use the transient model data to compare intervals within the Holocene when abrupt changes in
131 climate are known to have occurred in some regions (~8.2ka B.P. and ~4.2ka B.P.). These times
132 were recently adopted by the International Commission on Stratigraphy as the chronological
133 boundaries of the early, mid and late Holocene (Walker et al., 2012). We examine mean annual
134 surface temperature, annual precipitation and SSTs from the full-forcing experiment.

135 **2.1 Results**

136 First, we assess Holocene climate variability as simulated in the full-forcing experiment. Fig.
137 1 shows the time series of surface temperature and precipitation over the last past 13ka. It shows
138 cooling associated with the Younger Dryas, followed by Holocene warming, but also a brief
139 cooling episode from ~8500-8000 B.P. Thereafter the record exhibits strong multi-century scale
140 variability. Temperature and precipitation are positively correlated at this global scale. It is
141 tempting to associate the colder episodes with those identified by Wanner et al (2011) or by Bond
142 et al. (2001) but only a few of these are coincident in time.

143 The period 4.5ka-4.0ka BP was chosen for analysis, by subtracting the mean annual 2m air
144 temperatures, SSTs and precipitation from 4500-4000 years B.P. from the preceding period (4800-
145 4500 years B.P.). The spatial distribution of air temperature (Fig. 2a) shows that temperatures were
146 significantly colder over most of the extra-tropical northern hemisphere, but generally warmer in
147 the Tropics and in the southern hemisphere. The main exception is in northern South America,
148 which was cooler, and northern India and Pakistan, which were significantly warmer. Precipitation
149 decreased over almost all of the northern hemisphere, particularly in the Tropics where the ITCZ
150 shifted south, resulting in higher rainfall in the 0-20°S zonal band from 4500-4000 years B.P.
151 (Figure 2b). There was less precipitation over the northern part of China but more precipitation
152 over southern China, consistent with paleoclimate reconstructions that indicate a weaker East
153 Asian monsoon (Wang et al., 2005). This pattern is similar to some of the megadroughts that have
154 happened in recent centuries (Cook et al., 2010). Over other Asian monsoon regions, such as
155 India, there were also significant precipitation reductions during the second half of the 5th



156 millennium B.P., consistent with speleothem records that show a decline in Indian summer
157 monsoon rainfall over this period (Kathayat et al., 2017). Over Central America and the northern
158 edge of South America, conditions were also drier in the later period, but over the rest of South
159 America, and adjacent ocean regions, precipitation was higher due to a southward displacement of
160 the ITCZ; this pattern is supported by speleothem records of rainfall in Mexico and Brazil
161 (Lachniet et al., 2013; Bernal et al., 2016). The SST pattern shows significantly cooler
162 temperatures in the period 4500-4000 years B.P. over the North Atlantic. This cooling is centered
163 around 50°N (south of Iceland) and extends into the sub-Tropics on the eastern side of the sub-
164 tropical gyre. Slightly cooler temperatures are also found over the North Pacific (Fig. 2c). By
165 contrast, for most of the southern hemisphere there was a positive change in temperature. Rotated
166 EOF analysis on the global SST field shows the primary feature (in EOFs 1 and 2) to be the cooler
167 SSTs over the North Atlantic, with a shift around 4.5ka BP from a predominantly positive to a
168 generally negative pattern (Fig. 3). This is similar to an AMO-like pattern over the northern
169 Atlantic that has been identified in both instrumental and paleoclimatic records (Delworth and
170 Mann, 2000; Knudsen et al., 2011).

171 The same evaluation of changes in the 9th millennium B.P. was made by subtracting the
172 mean annual 2m air temperatures, SSTs and precipitation from 8800-8000 from the preceding
173 period (9200-8800 years B.P.). Air temperatures were significantly lower in the second period
174 over most of the northern hemisphere; only a zone from northern South America across to sub-
175 Saharan Africa and India was warmer in the second period (Fig. 4a). Almost the entire southern
176 hemisphere was warmer. Precipitation was less in the second period across all of the northern
177 hemisphere, especially along the ITCZ, which was displaced to the south. This resulted in an
178 increase in rainfall in a belt south of the Equator, across almost all of the Tropics (Fig. 4b). The
179 rest of the southern hemisphere was also slightly wetter. SSTs show a strong pattern of cooling
180 over the North Pacific, and the eastern North Atlantic, south of Iceland, extending around the
181 Atlantic sub-tropical gyre into the tropical Atlantic and Caribbean (Fig. 4c). Rotated EOFs show
182 that the anomalies in the North Atlantic and North Pacific dominate the first 3 EOFs (Fig. 5).

183 The spatial patterns of temperature changes, precipitation changes, and SST changes were
184 remarkably similar in the late 9th millennium as in the period leading up to the late 5th millennium
185 (Fig. 6). The major difference (Fig. 6a) is that SST changes over the subtropical Atlantic were
186 greater and the related changes across the northern hemisphere in the 9th millennium B.P. were



187 larger than in the 5th millennium. Similarly, the major changes in precipitation patterns were
188 comparable, but less pronounced from 4500-4000 years B.P. These similarities are somewhat
189 puzzling as the meltwater forcing sensitivity experiment clearly shows that the “8.2ka BP event”
190 was induced by a massive freshwater flux into the Atlantic whereas (as far as we know) no
191 comparable meltwater event occurred in the late Holocene so it seems unlikely that such forcing
192 was a factor driving the changes seen in the model output for 4500-4000 years B.P. A possible
193 explanation is that as summer insolation at high latitudes of the northern hemisphere declined over
194 the Holocene, a threshold was passed which led to cooler SSTs in the North Atlantic and a
195 consequent reduction in the Atlantic meridional overturning circulation (AMOC), with
196 teleconnections into the southern hemisphere. In our experiment, we examined just the 5th
197 millennium B.P., but it is possible that the changes seen in the latter half of the period were more
198 persistent, and typical of the rest of the Holocene (the Neoglacial). Indeed, there is much evidence
199 for cooler conditions and glacier expansion around the North Atlantic around this time (Solomina
200 et al., 2015). Thereafter, glaciers fluctuated but did not disappear again, indicating that a different
201 climate state prevailed. Fluctuations around these cooler mean conditions may be related to
202 internal centennial-scale ocean-atmosphere variability (cf. Wanner et al., 2011). This is distinctly
203 different from the period prior to 5000 years B.P. when many mountain regions were ice-free.
204 Further analysis of the TRACE21 simulations are needed to fully explore this matter.

205

206 **3. Conclusions**

207 Paleoclimate records have shown that cold and dry conditions persisting for several centuries
208 around 4.2ka BP over many different regions and these had devastating societal impacts. In this
209 study, the spatial patterns of temperature, precipitation, and corresponding circulation anomalies
210 during the latter part of the 9th and 5th millennia B.P. (4800-4500 versus 4500-4000 years B.P. and
211 9200-8800 versus 8800-8000 years B.P.) were compared based on model simulations. The
212 changes in climate during both periods were similar and characterized by significant temperature
213 and precipitation decreases over most of the northern hemisphere, but the southern hemisphere
214 was slightly warmer and wetter. In particular, the ITCZ was displaced to the south and monsoon
215 regions of the northern hemisphere were generally drier. On a regional scale, there was less
216 precipitation over the northern part of China but more precipitation over southern China, indicating
217 a reduced eastern Asian summer monsoon in the period 4500-4000 years B.P.



218 It is clear that the earlier period was strongly influenced by freshwater forcing in the North
219 Atlantic, but this can not explain the changes in the 5th millennium B.P. We speculate that long-
220 term changes in insolation related to precessional forcing led to cooling, which passed a threshold
221 around 4500 years B.P., leading to a reduction in the AMOC and associated teleconnections across
222 the globe. Based on widespread paleoclimatic evidence for the onset of neoglaciation (Solomina
223 et al., 2015), it seems clear that there was a fundamental shift in climate around this time.
224 Furthermore, those changes have persisted, with minor fluctuations, through to the present.
225 Interestingly, SSTs in the area of the North Atlantic where cooling was so prominent from 4500-
226 4000 years B.P. do show multi-century-scale oscillations for the remainder late Holocene, with
227 temperatures below the 4800-4500 years B.P. average for ~69% of the time (Fig. 7). Whether such
228 changes are also linked to hydrological anomalies elsewhere, as with the period 4500-4000 years
229 B.P., is not known, but it seems likely, given the large-scale coherent link between temperature
230 and precipitation that is apparent in Fig. 1. Whether such fluctuations reflect internal centennial-
231 scale ocean-atmosphere variability, or external forcing (explosive volcanic eruptions and/or solar
232 irradiance forcing) is also not known. Further studies of the role of external forcing are needed to
233 provide a better understanding of such mechanisms (cf. Ottera et al., 2010; Gupta and Marshall,
234 2018). Nevertheless, we conclude from the model simulations that the “4.2ka B.P. event” was
235 simply one of several late Holocene multi-century fluctuations that were embedded in a longer-
236 term, lower frequency change in climate resulting from orbital forcing.

237

238 **Acknowledgements**

239 This research was jointly supported by the National Key Research and Development Program of
240 China (Grant No. 2016YFA0600401), the National Natural Science Foundation of China (Grant
241 No. 41501210, Grant No. 41420104002, Grant No. 41671197, and Grant No. 41631175), the
242 Jiangsu Province Natural Science Foundation (Grant No. BK20150977), Top-notch Academic
243 Programs Project of Jiangsu Higher Education Institutions (Grant No. PPZY2015B115), and the
244 Priority Academic Development Program of Jiangsu Higher Education Institutions (Grant No.
245 164320H116). It also received support from U.S. NSF grant PLR-1417667 to the University of
246 Massachusetts. TraCE-21ka was made possible by the DOE INCITE computing program, and
247 supported by NCAR, the NSF P2C2 program, and the DOE Abrupt Change and EaSM programs.

248 **References:**



- 249 Alley, R.B., and Agustsdottir, A.M.: The 8k event: cause and consequences of a major Holocene
250 abrupt climate change, *Quaternary Science Reviews*, 24, 1123–1149, 2005.
- 251 Bernal, J.P., Cruz, F.W., Strikis, N.M., Wang, X., Deininger, M., Catunda, M.C.A., Ortega-
252 Obregón, C., Cheng, H., Edwards, R.L. and Auler, A.S.: High-resolution Holocene South
253 American monsoon history recorded by a speleothem from Botuverá Cave, Brazil, *Earth and
254 Planetary Science Letters*, 450, 186-196, 2016.
- 255 Bianchi, G., and McCave, I.N.: Holocene periodicity in north Atlantic climate and deep ocean flow
256 south of Iceland, *Nature*, 397, 515–518, 1999.
- 257 Bond, G., Kromer, B., Beer, J., Muscheler, R., Evans, M.N., Showers, W., Hoffmann, S., Lotti-
258 bond, R., Hajdas, I. and Bonani, G.: Persistent solar influence on North Atlantic climate during
259 the Holocene, *Science* 294, 2130-2136, 2001.
- 260 Booth, R. K., Jackson, S. T., Forman, S. L., Kutzbach, J. E., Bettis III, E. A., Kreig, J., and Wright,
261 D. K.: A severe centennial-scale drought in mid-continental North America 4200 years ago and
262 apparent global linkage, *The Holocene*, 15, 321-328, 2005.
- 263 Burns, S.J.: Speleothem records of changes in tropical hydrology over the Holocene and possible
264 implications for atmospheric methane, *The Holocene*, 21, 735-741, 2011.
- 265 Clarke, G.K.C., Leverington, D.W., Teller, J.T., and Dyke, A.S.: Paleohydraulics of the last
266 outburst flood from glacial Lake Agassiz and the 8200 BP cold event, *Quaternary Science
267 Reviews*, 23, 389–407, 2004.
- 268 Cook, E. R., Anchukaitis, K. J., Buckley, B. M., D’Arrigo, R. D., Jacoby, G. C., and Wright, W.
269 E.: Asian monsoon failure and megadrought during the last millennium, *Science*, 328, 486-489,
270 2010.
- 271 Deininger, M., McDermott, F., Mudelsee, M., Werner, M., Frank, N., Mangini, A.: Coherency of
272 late Holocene European speleothem $\delta^{18}O$ records linked to North Atlantic Ocean circulation,
273 *Climate. Dynamics*, 49, 595-618, 2017.
- 274 Delworth, T.L. and Mann, M.E.: Observed and simulated multidecadal variability in the Northern
275 Hemisphere, *Climate Dynamics*, 16, 661-676, 2000.
- 276 Finkenbinder, M. S., Abbott, M. B., and Steinman, B. A.: Holocene climate change in
277 Newfoundland reconstructed using oxygen isotope analysis of lake sediment cores, *Global and
278 Planetary Change*, 143, 251-261, 2016.



- 279 Gupta, M. and Marshall, J.: The climate response to multiple volcanic eruptions mediated by
280 ocean heat uptake: damping processes and accumulation potential, *J. Climate*, 31, 8669-8687,
281 2018.
- 282 He, F.: Simulation transient climate evolution of the last deglaciation with CCSM3, PhD
283 dissertation, University of Wisconsin-Madison, 185pp, 2011.
- 284 He, F., Shakun, J. D., Clark, P. U., Carlson, A. E., Liu, Z., Otto-Bliesner, B. L., and Kutzbach J.
285 E.: Northern Hemisphere forcing of Southern Hemisphere climate during the last deglaciation,
286 *Nature*, 494, 81-85, 2013.
- 287 Kathayat, G., Cheng, H., Sinha, A., Yi, L., Li, X., Zhang, H., Li, H., Ning, Y. and Edwards, R.L.:
288 The Indian monsoon variability and civilization changes in the Indian subcontinent, *Science*
289 *Advances*, 3, e1701296, 2017.
- 290 Knudsen, M.F., Seidenkrantz, M.S., Jacobsen, B.H. and Kuijpers, A.: Tracking the Atlantic
291 Multidecadal Oscillation through the last 8,000 years, *Nature Communications*, 2, 178-185,
292 2011.
- 293 Lachniet, M.S., Asmerom, Y., Bernal, J.P., Polyak, V.J. and Vazquez-Selem, L.: Orbital pacing
294 and ocean circulation-induced collapses of the Mesoamerican monsoon over the past 22,000
295 y, *Proceedings of the National Academy of Sciences*, 110, 9255-9260, 2013.
- 296 LeGrande, A.N., Schmidt, G.A., Shindell, D.T., Field, C.V., Miller, R.L., Koch, D.M., Faluvegi,
297 G. and Hoffmann, G.: Consistent simulations of multiple proxy responses to an abrupt climate
298 change event, *Proceedings of the National Academy of Sciences*, 103, 837-842, 2006.
- 299 Liu, Z., Zhu, J., Rosenthal, Y., Zhang, X., Otto-Bliesner, B.L., Timmermann, A., Smith, R.S.,
300 Lohmann, G., Zheng, W. and Timm, O.E.: The Holocene temperature conundrum, *Proceedings*
301 *of the National Academy of Sciences*, 111, E3501-E3505, 2014a.
- 302 Liu, Z., Yoshimura, K., Bowen, G. J., Buening, N. H., Risi, C., Welker, J. M., and Yuan, F.:
303 Paired oxygen isotope records reveal modern North American atmospheric dynamics during
304 the Holocene, *Nature Communications*, 5, 3701, DOI: 10.1038/ncomms4701, 2014b.
- 305 Marcott, S.A., Shakun, J.D., Clark, P.U., and Mix, A.C.: A reconstruction of regional and global
306 temperature for the past 11,300 years, *Science*, 339, 1198-1201, 2013.
- 307 McManus, J.F., Francois, R., Gherardi, J.-M., Keigwin, L. D., and Brown-Leger, S.: Collapse and
308 rapid resumption of Atlantic meridional circulation linked to deglacial climate changes, *Nature*,
309 428, 834-837, 2004.



- 310 Ottera, O. H., Bentsen, M., Drange, H., and Suo, L.: External forcing as a metronome for Atlantic
311 multidecadal variability, *Nature Geoscience*, 3, 688-694, 2010.
- 312 Otto-Bliesner, B. L., Brady, E. C., Clauzet, G., Tomas, R., Levis, S., and Kothavala, Z.: Last
313 Glacial Maximum and Holocene climate in CCSM3, *J. Climate*, **19**, 2526-2544, 2006.
- 314 Risebrobakken, B., Jansen, E., Andersson, C., Mjelde, E., Hevrøy, K.: A high resolution study of
315 Holocene paleoclimatic and paleoceanographic changes in the Nordic Seas, *Paleoceanography*,
316 18, 1–14, 2003.
- 317 Solomina, O.N., Bradley, R.S., Hodgson, D.A., Ivy-Ochs, S., Jomelli, V., Mackintosh, A.N.,
318 Nesje, A., Owen, L.A., Wanner, H., Wiles, G.C. and Young, N.E.: Holocene glacier
319 fluctuations, *Quaternary Science Reviews*, 111, 9-34, 2015.
- 320 Staubwasser, M., and Weiss, H.: Holocene climate and cultural evolution in late prehistoric-early
321 historic West Asia. *Quaternary Research*, 66, 372-387, 2006.
- 322 Tan, L., Cai, Y., Cheng, H., Edwards, L. R., Gao, Y., Xu, H., Zhang, H., and An, Z.: Centennial-
323 to decadal- scale monsoon precipitation variations in the upper Hanjiang River region, China
324 over the past 6650 years, *Earth and Planetary Science Letters*, 482, 580-590, 2018.
- 325 Thompson, L. G., Mosley-Thompson, E., Davis, M. E., Henderson, K. A., Brecher, H. H.,
326 Zagorodnov, V. S., Mashiotta, T. A., Lin, P.-N., Mikhalevko, V. N., Hardy, D. R., and Beer, J.:
327 Kilimanjaro ice core records: evidence of Holocene climate change in tropical Africa, *Science*,
328 298, 589-593, 2002.
- 329 Walker, M.J., Berkelhammer, M., Björck, S., Cwynar, L.C., Fisher, D.A., Long, A.J., Lowe, J.J.,
330 Newnham, R.M., Rasmussen, S.O. and Weiss, H.: Formal subdivision of the Holocene
331 Series/Epoch: a Discussion Paper by a Working Group of INTIMATE (Integration of ice-core,
332 marine and terrestrial records) and the Subcommission on Quaternary Stratigraphy
333 (International Commission on Stratigraphy), *Journal of Quaternary Science*, 27, 649-659, 2012.
- 334 Wang, S.: Holocene climate, *Advances in climate change research*, 5, 247-248, 2009a (in Chinese
335 with English abstract)
- 336 Wang, S.: Holocene cold events in the north Atlantic chronology and climatic impact, *Quaternary*
337 *Sciences*, 29, 1146-1153, 2009b (in Chinese with English abstract)
- 338 Wang, Y., Cheng, H., Edwards, L. R., He, Y., Kong, X., An, Z., Wu, J., Kelly, M. J., Dykoski, C.
339 A., and Li, X.: The Holocene Asian monsoon: links to solar changes and north Atlantic climate,
340 *Science*, 308, 854-857, 2005.



341 Weiss, H.: Megadrought, collapse, and resilience in late 3rd millennium BC Mesopotamia. In book:
342 Meller, H., Arz, H. W., Jung, R., and Risch, R., eds, 2200 BC – A climatic breakdown as a
343 cause for collapse of the Wold World? Halle: Landesmuseum fur Vorgeschichte, 35-52, 2015.

344 Weiss, H.: Global megadrought, societal collapse and resilience at 4.2-3.9 ka BP across the
345 Mediterranean and west Asia, PAGES Magazine, 24, 62-63, 2016.

346

347

348

349

350

351

352

353

354

355

356

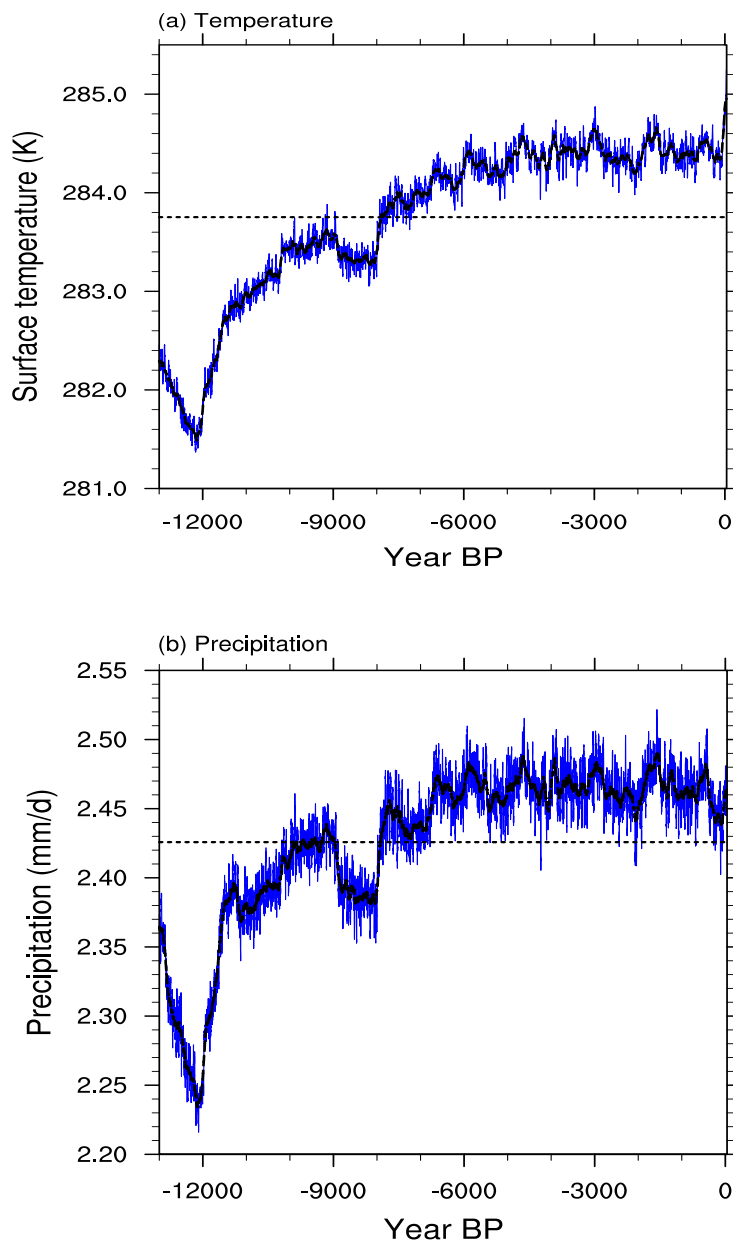
357

358

359

360

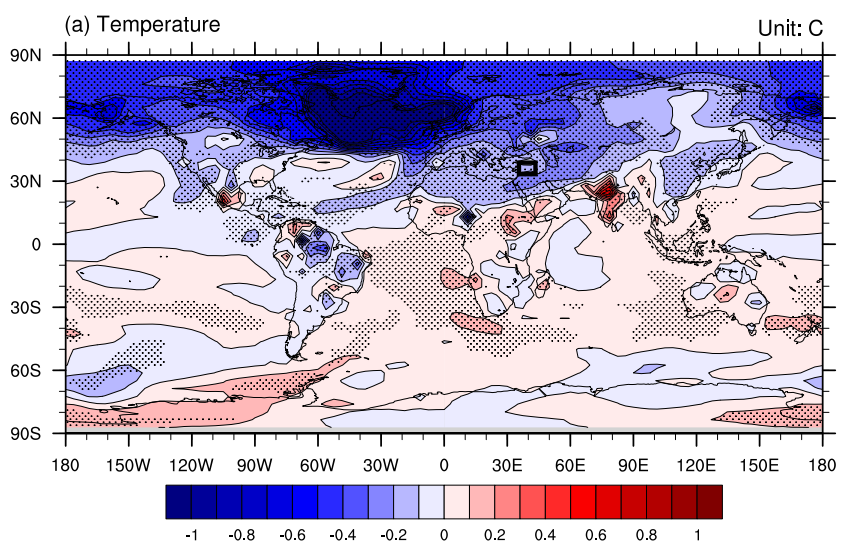
361



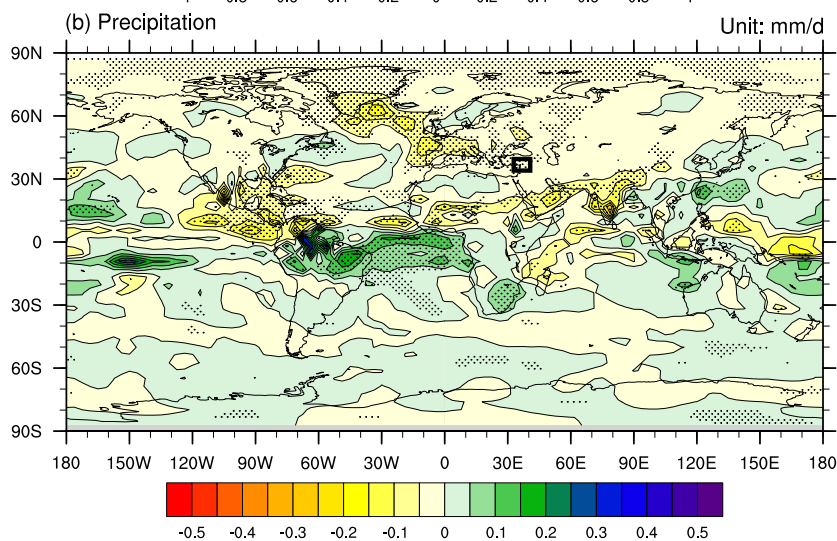
362

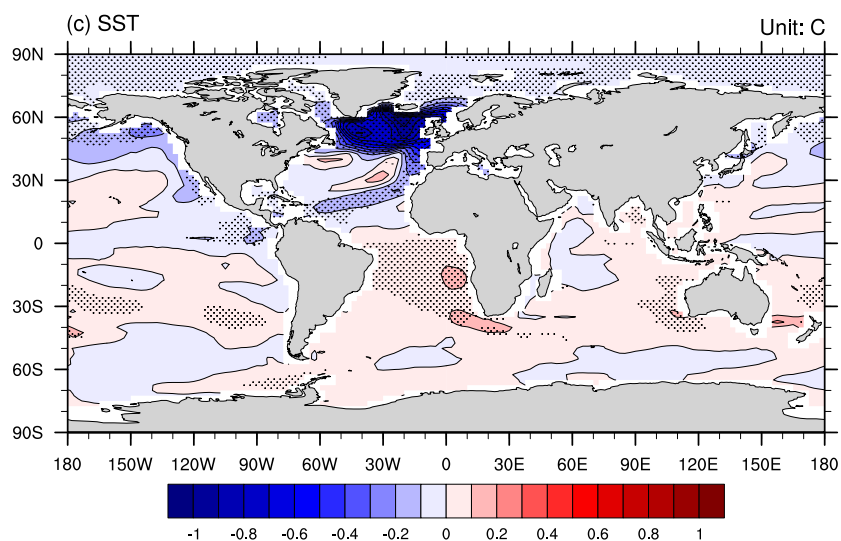
363
364
365
366
367
368
369

Figure 1. The 10-year running averaged (blue line) and 100-year running averaged (black line) northern hemisphere average surface temperature and precipitation over the last 13ka years from the all-forcing experiment.



370
371
372
373
374
375
376
377
378
379
380
381
382
383
384
385
386
387
388
389
390
391
392
393
394
395
396





397

398

399

400 **Figure 2.** The changes of surface temperature (a, unit: °C), precipitation (b, unit: mm/day), and

401 SST (c, unit: °C) after 4.5ka BP (between 4500-4000ka BP and 4800-4500ka BP)

402

403

404

405

406

407

408

409

410

411

412

413

414

415

416

417

418

419

420

421

422

423

424

425

426

The rectangles indicate the region with major dry-farming settlement abandonments shown in Fig. 2 of Weiss (2016)



427
428
429
430
431
432
433
434
435
436
437
438
439
440
441
442
443
444
445
446
447
448
449
450
451
452
453
454
455
456
457
458
459
460
461
462
463
464
465
466
467
468
469
470
471
472

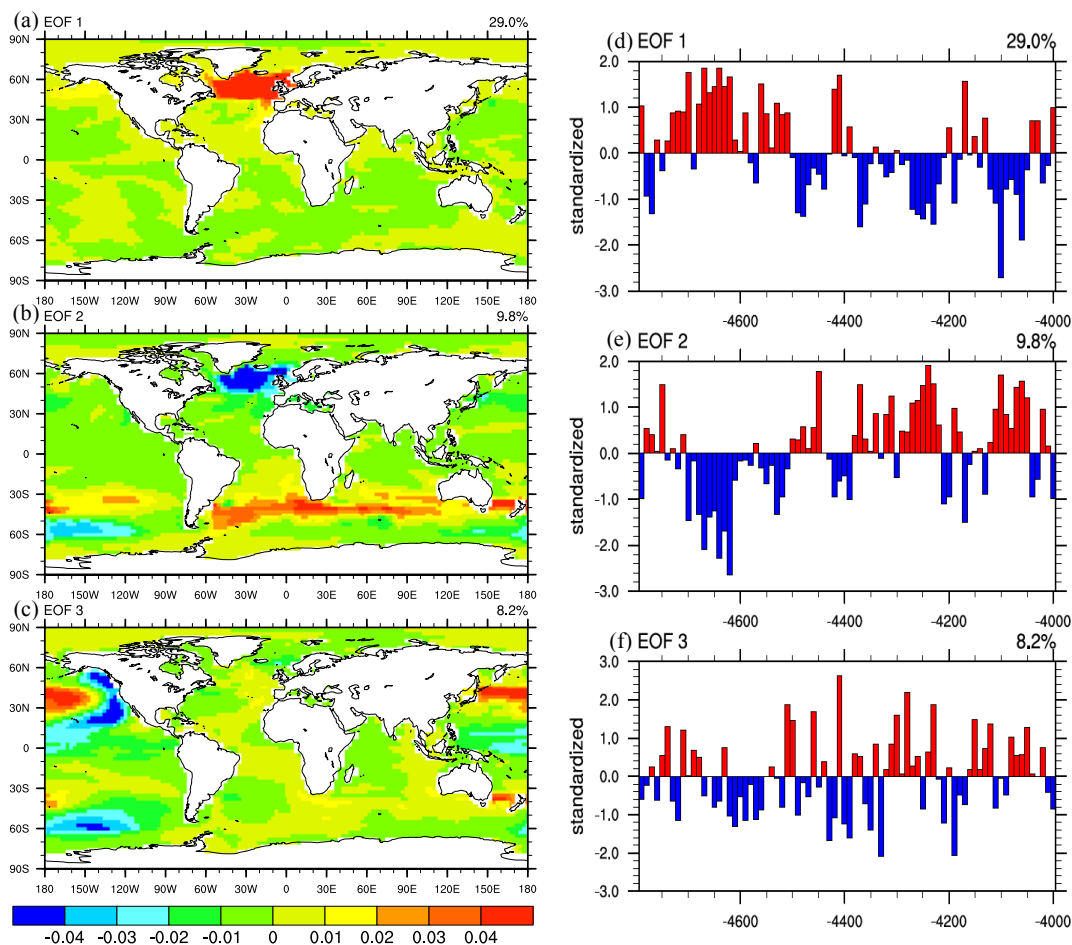
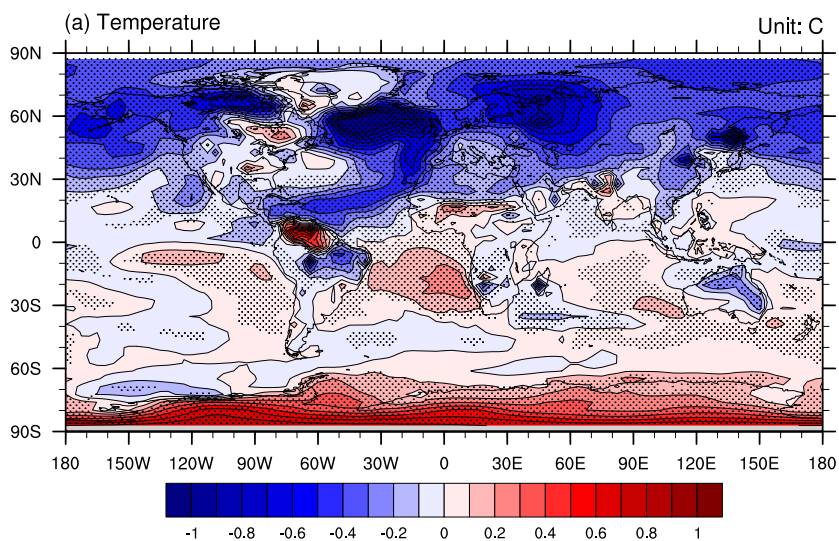


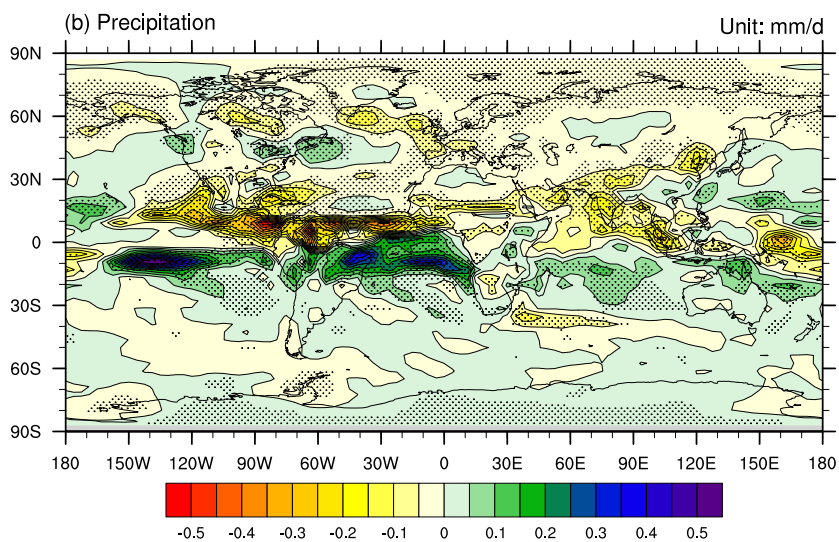
Figure 3. The first three patterns (a-c) and principal components (d-f) of rotated EOF modes on the SST over the period 4800-4000ka BP.



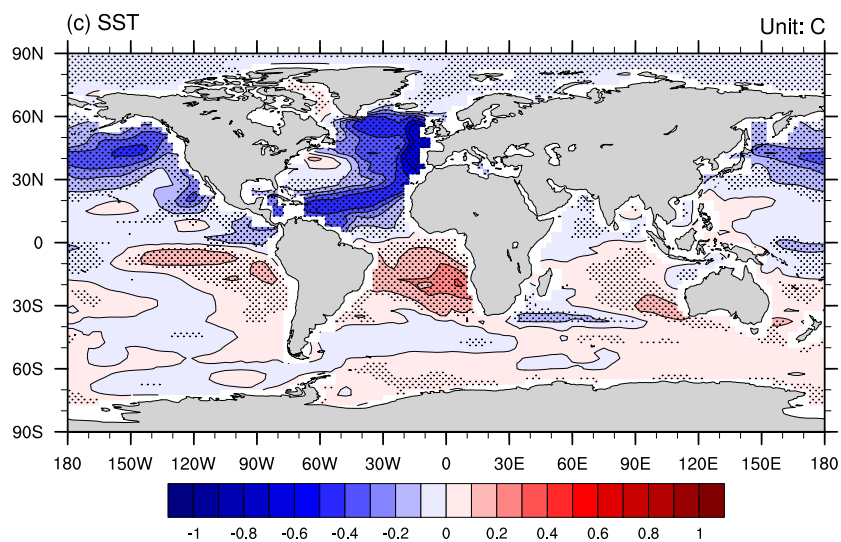
473
474



475



476



477
478
479
480
481
482
483
484
485
486
487
488
489
490
491
492
493
494
495
496
497
498
499
500
501
502
503
504
505
506

Figure 4. The changes of surface temperature (a), (a, unit: °C), precipitation (b, unit: mm/day), and SST (c, unit: °C) after 8.8ka BP (between 8800-8000ka BP and 9200-8800ka BP)



507
508
509
510
511
512
513
514
515
516
517
518
519
520
521
522
523
524
525
526
527
528
529
530
531
532
533
534
535
536
537
538
539
540
541
542
543
544
545
546
547
548
549
550
551
552

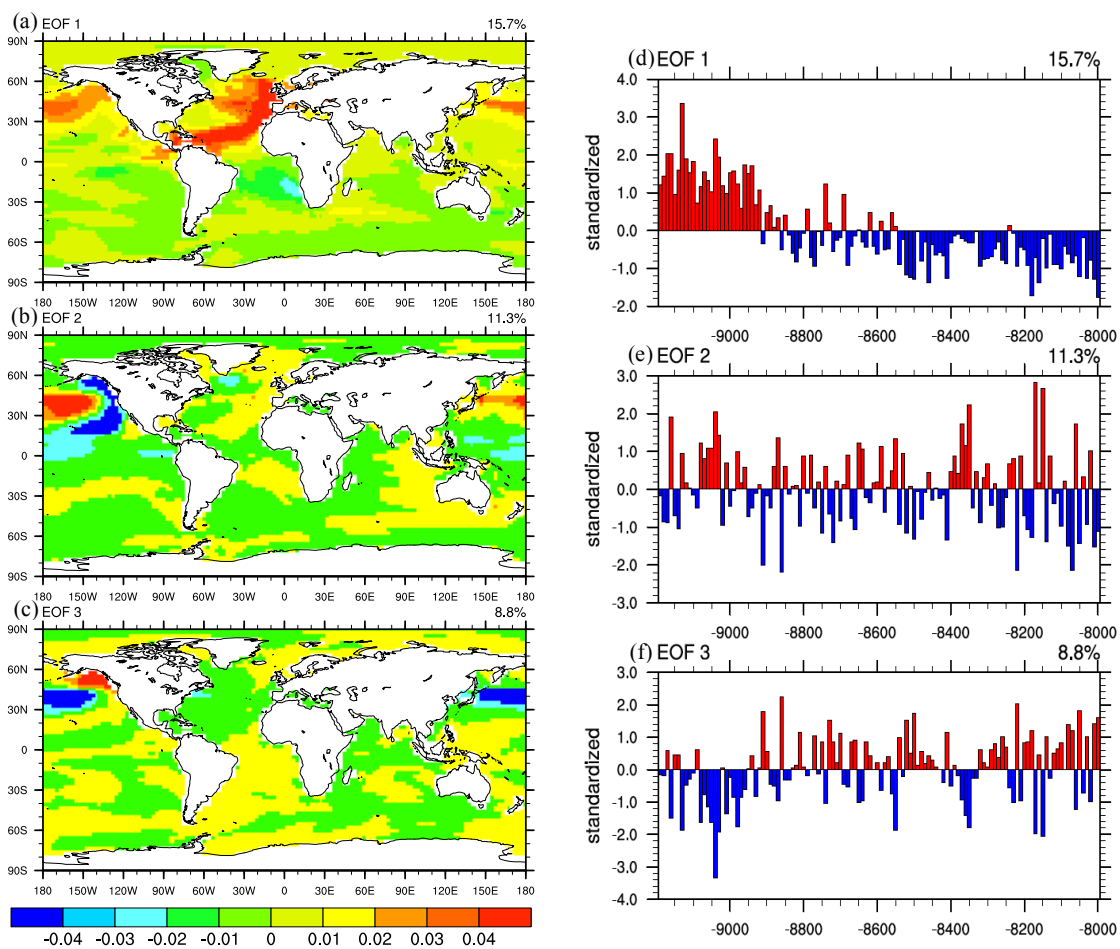
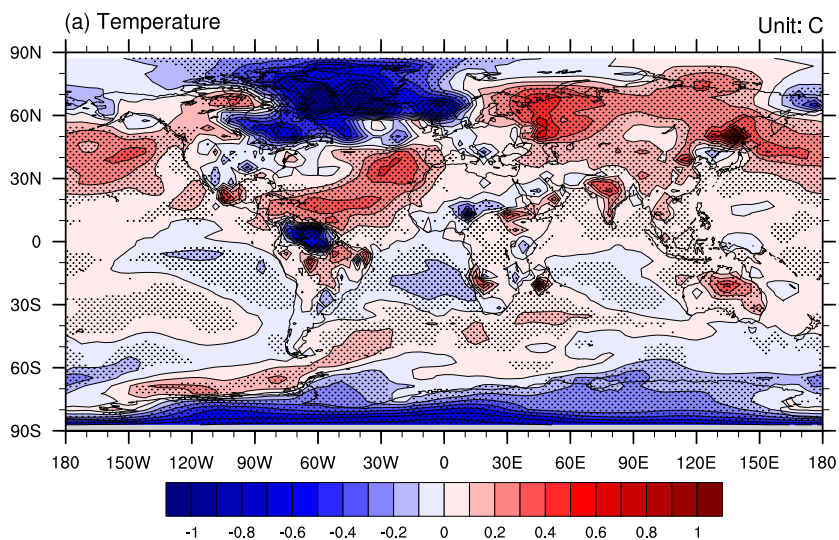


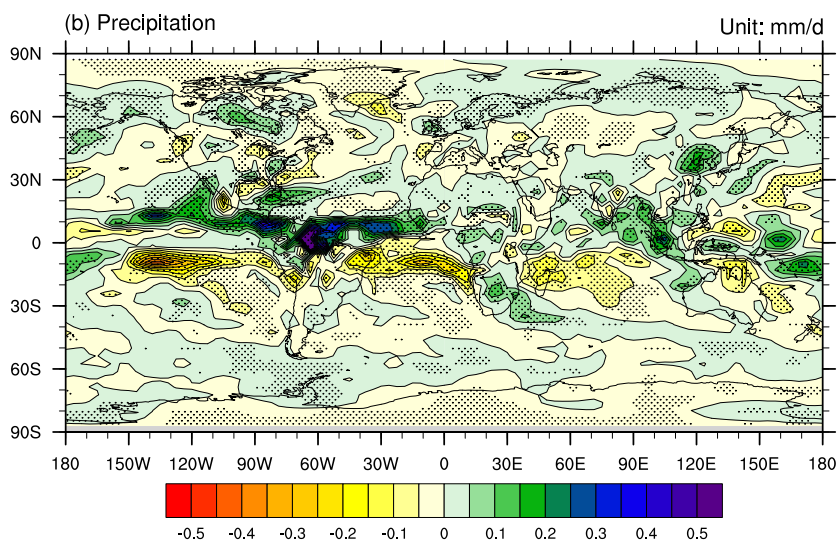
Figure 5. The first three patterns (a-c) and principal components (d-f) of rotated EOF modes on the SST over the period 9200-8000ka BP.



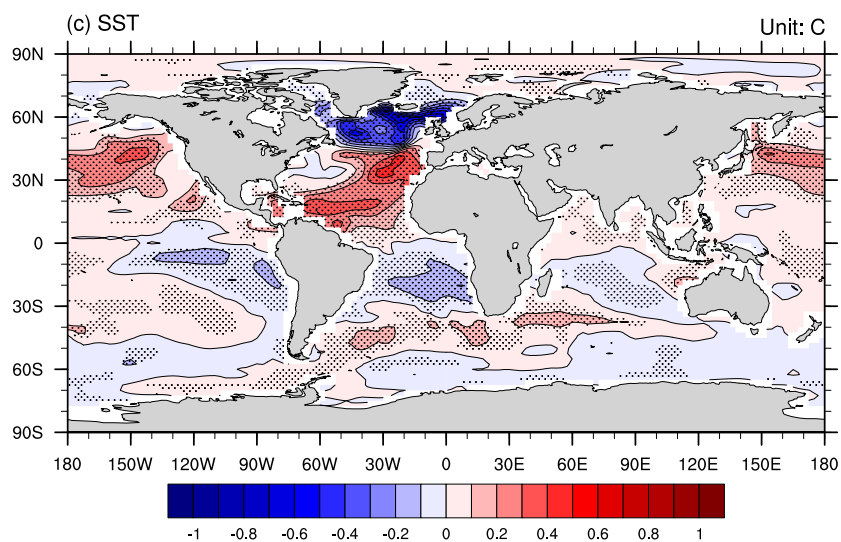
553
554
555



556
557

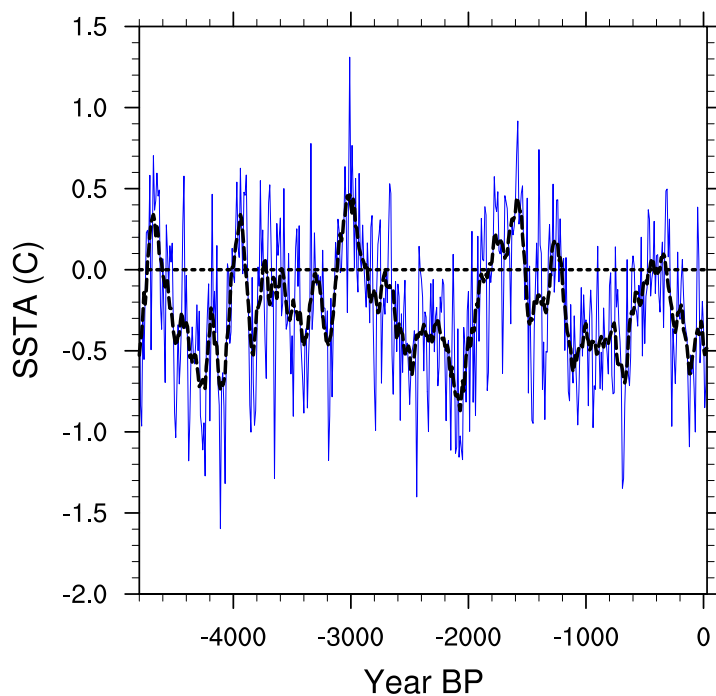


558
559



560
561
562
563
564
565
566
567

Figure 6. The differences between changes of surface temperature (a), (a, unit: °C), precipitation (b, unit: mm/day), and SST (c, unit: °C) of the 5th millennium BP and 9th millennium BP periods shown in Figures 2 and 4.



568

569

570

Figure 7. SSTs in the area of the North Atlantic shown in dark blue (40-60 °N, 7.5-60 °W) on Figure 2c, plotted as anomalies from the mean for 4800-4500 years B.P. ~69% of the time, temperatures in this region were below the mean.

571

572

573